# 3-node Basic Displacement Functions in Analysis of Non-Prismatic Beams

A. Modarakar Haghighi [1*], M. Zakeri [2], R. Attarnejad [3]

*1. School of Civil Engineering, College of Engineering, University of Tehran, Tehran P.O. Box 11365-4563, Iran*
*2. Assistant Professor, Faculty of Mechanical Engineering, University of Kashan, Kashan, Iran*
*3. MS Graduate, Faculty of Mechanical Engineering, University of Kashan, Kashan, Iran*

## Abstract

Purpose– Analysis of non-prismatic beams has been focused of attention due to wide use in complex structures such as aircraft, turbine blades and space vehicles. Apart from aesthetic aspect, optimization of strength and weight is achieved in use of this type of structures. The purpose of this paper is to present new shape functions, namely 3-node Basic Displacement Functions (BDFs) for derivation of structural matrices for general non-prismatic Euler-Bernoulli beam elements. Design/methodology/approach– Static analysis and free transverse vibration of non-prismatic beams are extracted studied from a mechanical point of view. Following structural/mechanical principles, new static shape functions are in terms of BDFs, which are obtained using unit-dummy-load method. All types of cross-sections and cross-sectional dimensions of the beam element could be considered in this method. Findings– According to the outcome of static analysis, it is verified that exact results are obtained by applying one or a few elements. Furthermore, it is observed that results from both static and free transverse vibration analysis are in good agreement with the previous published once in the literature. Research limitations/implications– The method can be extended to structural analysis of curved and Timoshenko beams as well as plates and shells. Furthermore, exact dynamic shape functions can be derived using BDFs by solving the governing equation for transverse vibration of beams. Originality/value– The present investigation introduces new shape functions, namely 3-node Basic Displacement Functions (BDFs) extended from 2-node functions, and then compares its performance with previous element.

**Keywords:** *3-node basic displacement functions, free transverse vibration, non-prismatic beam, shape functions, static analysis.*

## 1. Introduction

Analysis of beams has been focused of attention due to wide use in complex structures such as aircraft, turbine blades and space vehicles. Apart from aesthetic aspect, optimization of strength and weight is achieved in use of this type of structures. Consequently, exact static and dynamic analyses of these members become more significant. Through the years, many researchers devoted their contributions to either formulating new

---

[*] Corresponding Author, Tel.: +98 9127935898; Fax: +98 21 22323705, Email:: za57190@gmail.com

elements or enhancing the existing approximate elements. Gunda and Ganguli [1] proposed new rational shape functions for finite-element analysis of rotating tapered beams through solving the static part of the governing differential equation.

Caruntu [2] utilized hyper-geometric functions to study free vibration of cantilever beams with parabolic thickness variation. Gallagher and Lee [3] derived approximate structural matrices for dynamic and instability analyses of non-uniform beams. Karabalis and Beskos [4] proposed a new element for static, stability and dynamic analyses of linearly tapered beams. Their method employs exact flexural and axial stiffness matrices but approximate consistent mass and geometric stiffness matrices. Eisenberger and Reich [5] obtained an approximate stiffness matrix for beams whose depth or width varied as an overall polynomial along beam length using shape functions of uniform beams.

Subsequently, Eisenberger [6, 7] derived exact stiffness matrices for beams with general variation of depth/width via a series solution of the governing equation. Banerjee and Williams [8] obtained exact dynamic stiffness matrix in terms of Bessel's functions for a class of tapered members whose area and moment of inertia vary as any arbitrary integer powers n and n+2, respectively. Mou et al. [9] computed the exact dynamic stiffness matrix in terms of hyper geometric functions for beams whose area and moment of inertia vary in accordance with any two arbitrary real-number powers.

Studying the effects of reduced beam section frame elements on stiffness of moment frames, Chambers et al. [10] derived stiffness matrix of a two-dimensional frame element with radius flange reductions, which is symmetric about the centroid of the element using virtual work theories. Kim and Engelhardt [11] proposed a new non-prismatic beam element for modeling the elastic behavior of steel beams with reduced beam section connections. Ece et al. [12] performed vibration analysis by analytical solving of governing differential equation of free vibration of beams with exponentially varying width and constant height.

In recent years, several researchers have focused on vibration of non-prismatic beams by solving the governing equation of motion via application of different numerical techniques, i.e. Frobenius method [13-15], Chebyshev series [16], Raleigh-Ritz method [17] and differential transform method [18-28]. The analysis of structural members generally includes two methods, namely displacement-based method (stiffness method) and flexibility method (force method). Equilibrium of forces, compatibility of displacements/strains and constitutive law of materials are the basic three essential relations that should be satisfied for the exact solution in any structural analysis. Additionally, an extra hypothesis in the displacement field is usually imposed in addition to these three fundamental relations. Generally, the equilibrium equations are satisfied only in certain points of elements, such as integration points. Thus the stiffness method is approximate in nature; however, the generality of this method seems to be the great advantage. In contrary, the flexibility method ensures accurate structural analysis and satisfies the equilibrium equations at any interior point of the element. However, the application of this method usually requires complicated and tedious calculations.

In this study, a simple flexibility-based formulation is proposed for derivation of structural matrices for general non-prismatic Euler-Bernoulli beam elements. This concept was, firstly, proposed by Attarnejad [29-31]. Basic Displacement Functions (BDFs) are presented; and 3-node method is introduced extending from 2-node method. Exact shape functions are obtained from these BDFs. There are two categories of BDFs, namely static BDFs, which are derived based on static deformations [31-33] and dynamic BDFs, which are derived assuming dynamic deformations [34-37]. The BDFs presented are obtained on the basis of static deformations. The advantage of this method is that it does not involve any cumbersome mathematical/numerical calculation; it also covers most of the engineering problems concerning non-prismatic beams.

The basic elements of a paper in the order in which they should appear are: Title, Authors, Affiliations, Abstract, Keywords, Main text, Acknowledgments, Appendix, and References. Authors should submit their manuscript by the Journal website. Electronic submission substantially reduces the editorial processing, reviewing and publication times. Please attach

your covering letter providing assurance that the manuscript has neither been published nor submitted for publication elsewhere. The corresponding author will be noted of the acceptance of their paper by the editor.

The authors of accepted paper with conditional acceptance are required to address the comments of the referees suitably in their revised paper and in their final full paper and address their revisions properly in a separate file and upload it to the Journal website. Authors will be asked, upon acceptance of an article, to transfer copyright of the article to the publisher. This will ensure the widest possible dissemination of the information under copyright laws. This form can be uploading from the Journal website. The Editors reserve the right to return manuscripts that do not conform to the instructions for manuscripts preparation or papers that do not fit the scope Journal, prior to referring.

## 2. Basic Displacement Functions

BDFs are mathematical functions, which derived from fundamental mechanical concepts. For definition of BDFs, consider a beam which one of its nodes is free; the others are clamped. A BDFs is defined as nodal displacement of the free node due to unit load at the distance $x$. For a 3-node beam, BDFs are introduced as:

$b_{wm}$ : vertical displacement of the m-th node due to unit load at distance $x$ when the beam is clamped at the others.

$b_{\theta m}$ : angle of rotation of the m-th node due to unit load at distance $x$ when the beam is clamped at the others.

(where m=1, 2, 3)

$b_{w1}, b_{\theta 1}, b_{w2}, b_{\theta 2}, b_{w3}, b_{\theta 3}$ are showed in Figure 1.
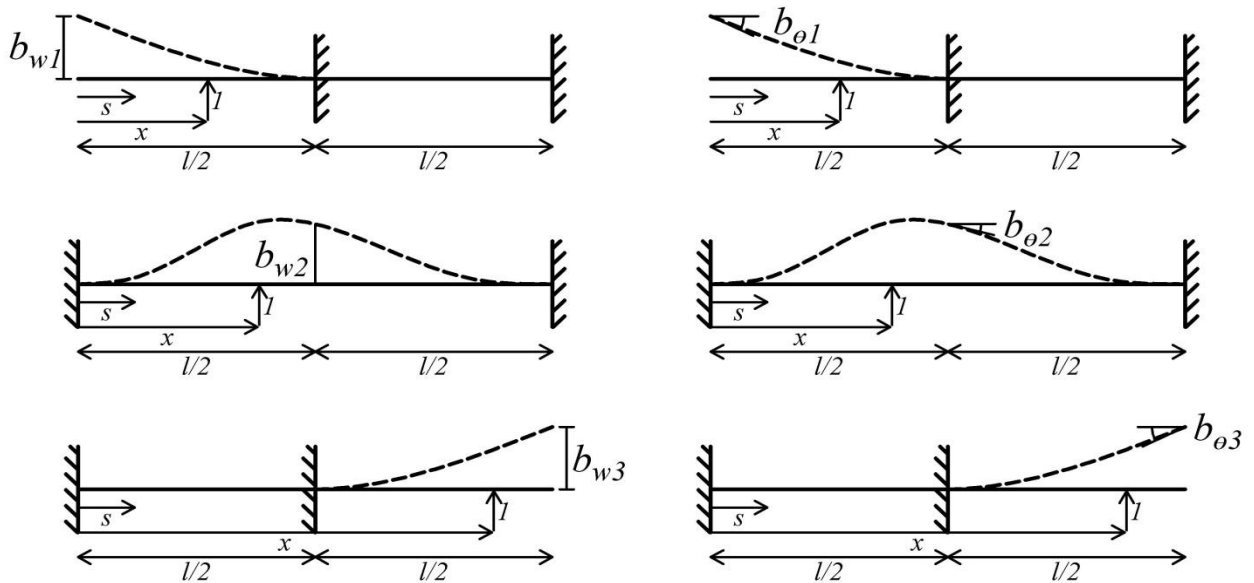


**Fig. 1. Definitions of BDFs**

For 1st and 3th nodes:

$$b_{w1}(x) = sg(\frac{l}{2} - x) \int_x^{1/2} \frac{s(s-x)}{EI(s)} ds \qquad (1)$$

$$b_{\theta 1}(x) = sg(\frac{l}{2} - x) \int_x^{1/2} \frac{-(s-x)}{EI(s)} ds \qquad (2)$$

$$b_{w3}(x) = sg(x - \frac{l}{2}) \int_{1/2}^x \frac{(l-s)(x-s)}{EI(s)} ds \qquad (3)$$

$$b_{\theta 3} = sg(x - \frac{l}{2}) \int_{1/2}^x \frac{-(s-x)}{EI(s)} ds \qquad (4)$$

where:

$$sg(y) = \begin{cases} 0 & y < 0 \\ 1 & y \geq 0 \end{cases}$$

For the mid-node:

By solving the geometry equations, reactions are determined due to unit load at distance $x$ (Fig. 2):

$$R_1 = \frac{\int_x^l \frac{s(s-x)}{EI(s)}ds \int_0^l \frac{1}{EI(s)}ds - \int_x^l \frac{(s-x)}{EI(s)}ds \int_0^l \frac{s}{EI(s)}ds}{\int_0^l \frac{s^2}{EI(s)}ds \int_0^l \frac{1}{EI(s)}ds - \int_0^l \frac{s}{EI(s)}ds \int_0^l \frac{s}{EI(s)}ds} \qquad (5)$$

$$M_1 = \frac{\int_x^l \frac{(s-x)}{EI(s)}ds \int_0^l \frac{s^2}{EI(s)}ds - \int_x^l \frac{s(s-x)}{EI(s)}ds \int_0^l \frac{s}{EI(s)}ds}{\int_0^l \frac{s}{EI(s)}ds \int_0^l \frac{s}{EI(s)}ds - \int_0^l \frac{s^2}{EI(s)}ds \int_0^l \frac{1}{EI(s)}ds} \qquad (6)$$
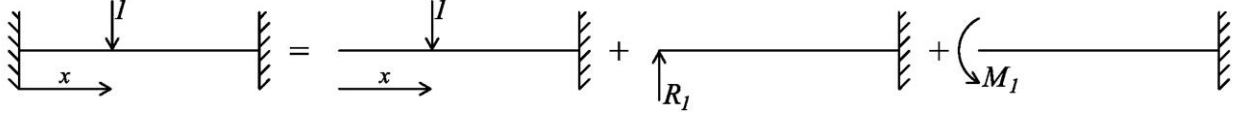


**Fig. 2. General beam with unit load at distance $x$ decomposed into isostatic structures**

which moment through the beam can be obtained:

$$M_s = R_1 s - M_1 - H(s-x)(s-x) \qquad (7)$$

Following similar procedure, we can obtain support reactions due to unit load and unit moment at distance $l/2$ (Fig. 3).
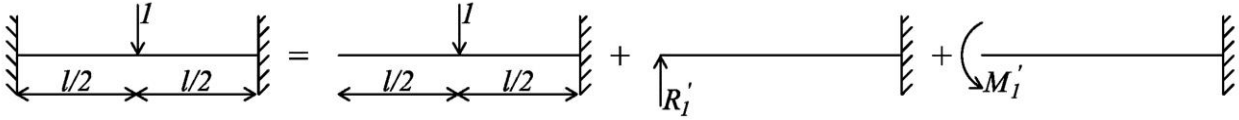


**Fig. 3. General beam with unit load at distance $l/2$ divided into isostatic structures**

$$R_1' = \frac{\int_{l/2}^l \frac{s(s-\frac{l}{2})}{EI(s)}ds \int_0^l \frac{1}{EI(s)}ds - \int_{l/2}^l \frac{(s-\frac{l}{2})}{EI(s)}ds \int_0^l \frac{s}{EI(s)}ds}{\int_0^l \frac{s^2}{EI(s)}ds \int_0^l \frac{1}{EI(s)}ds - \int_0^l \frac{s}{EI(s)}ds \int_0^l \frac{s}{EI(s)}ds} \qquad (8)$$

$$M_1' = \frac{\int_{l/2}^l \frac{(s-\frac{l}{2})}{EI(s)}ds \int_0^l \frac{s^2}{EI(s)}ds - \int_{l/2}^l \frac{s(s-\frac{l}{2})}{EI(s)}ds \int_0^l \frac{s}{EI(s)}ds}{\int_0^l \frac{s}{EI(s)}ds \int_0^l \frac{s}{EI(s)}ds - \int_0^l \frac{s^2}{EI(s)}ds \int_0^l \frac{1}{EI(s)}ds} \qquad (9)$$

$$M_s' = R_1' s - M_1' - H(s-\frac{l}{2})(s-\frac{l}{2}) \qquad (10)$$

For unit moment (Fig. 4):
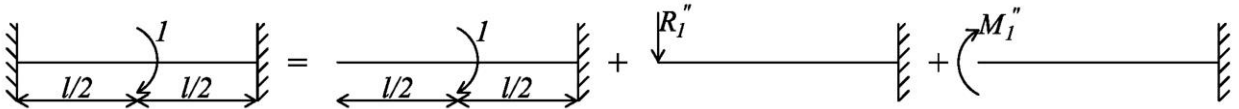


**Fig. 4. General beam with unit moment at distance $l/2$ divided into isostatic structures**

$$R_1'' = \frac{\int_{l/2}^l \frac{s}{EI(s)}ds \int_0^l \frac{1}{EI(s)}ds - \int_{l/2}^l \frac{1}{EI(s)}ds \int_0^l \frac{s}{EI(s)}ds}{\int_0^l \frac{s^2}{EI(s)}ds \int_0^l \frac{1}{EI(s)}ds - \int_0^l \frac{s}{EI(s)}ds \int_0^l \frac{s}{EI(s)}ds} \qquad (11)$$

$$M_1^{"} = \frac{\int_{1/2}^{l} \frac{1}{EI(s)} ds \int_0^l \frac{s^2}{EI(s)} ds - \int_{1/2}^{l} \frac{s}{EI(s)} ds \int_0^l \frac{s}{EI(s)} ds}{\int_0^l \frac{s}{EI(s)} ds \int_0^l \frac{s}{EI(s)} ds - \int_0^l \frac{s^2}{EI(s)} ds \int_0^l \frac{1}{EI(s)} ds}$$ (12)

$$M_s^{"} = M_1^{"} - R_1^{"} s + H(s - \frac{l}{2})$$ (13)

Finally BDFs of the mid-node are:

$$b_{w2} = \int_0^l \frac{M_s M_s'}{EI(s)} ds$$ (14)

$$b_{\theta 2}(x) = \int_0^l \frac{M_s M_s''}{EI(s)} ds$$ (15)

Regarding the reciprocal theorem, each BDF has equivalent definitions, which are as follows:

$b_{wm}$: vertical displacement of a point at distance $x$ due to unit load at the m-th node when the beam is clamped at the others.

$b_{\theta m}$: angle of rotation of a point at distance $x$ due to unit moment at the m-th node when the beam is clamped at the others.

$b_{w1}, b_{\theta 1}, b_{w2}, b_{\theta 2}, b_{w3}, b_{\theta 3}$ are showed in Figure 5.
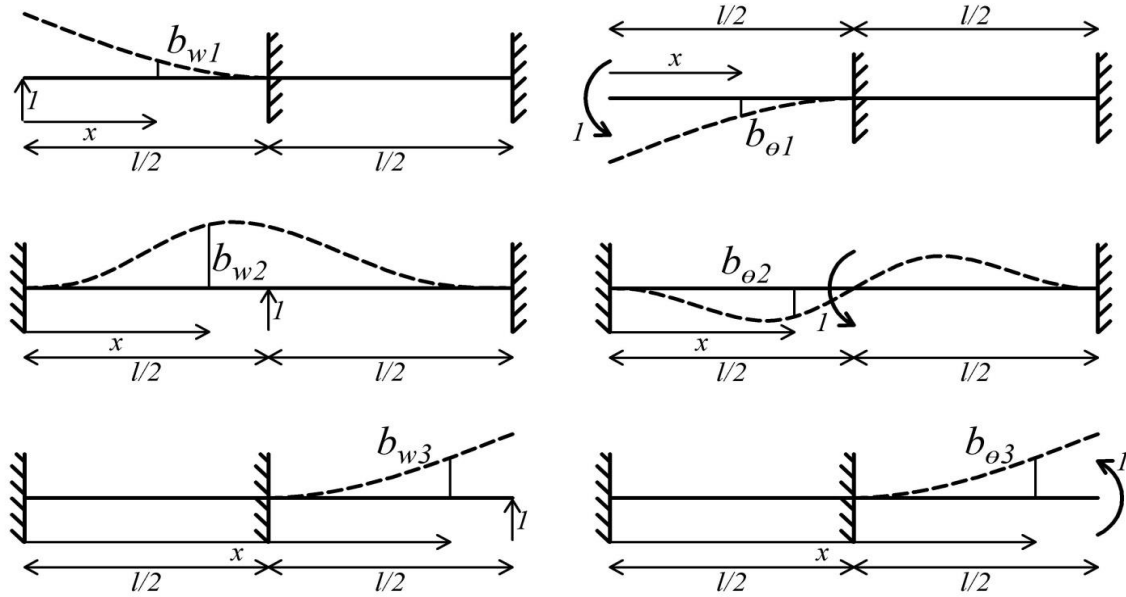


**Fig. 5. Equivalent definitions of BDFs**

Considering the equivalent definitions of BDFs, the angles of rotation and curvature of the beam corresponding to the BDF are respectively indicated in the first and second derivatives of each BDF. The required derivatives could be either obtained using principle of structural analysis or calculated using the Leibniz formula:

$$\frac{\partial}{\partial s} \int_{f_1(s)}^{f_2(s)} g(s,t) dt = \int_{f_1(s)}^{f_2(s)} \frac{\partial g(s,t)}{\partial s} dt + \frac{\partial f_2(s)}{\partial s} g(s, f_2(s)) - \frac{\partial f_1(s)}{\partial s} g(s, f_1(s))$$

Moreover, the flexibility matrix is obtained as:

$$F_{11} = \begin{bmatrix} b_{w1}(0) & b_{\theta 1}(0) \\ \frac{db_{w1}}{dx}\Big|_{x=0} & \frac{db_{\theta 1}}{dx}\Big|_{x=0} \end{bmatrix}$$ (16)

$$F_{22} = \begin{bmatrix} b_{w2}(\frac{l}{2}) & b_{\theta 2}(\frac{l}{2}) \\ \frac{db_{w2}}{dx}\Big|_{x=\frac{l}{2}} & \frac{db_{\theta 2}}{dx}\Big|_{x=\frac{l}{2}} \end{bmatrix}$$ (17)

$$F_{33} = \begin{bmatrix} b_{w3}(l) & b_{\theta3}(l) \\ \dfrac{db_{w3}}{dx}\bigg|_{x=l} & \dfrac{db_{\theta3}}{dx}\bigg|_{x=l} \end{bmatrix} \qquad (18)$$

The Nodal stiffness matrix can be obtained by inverting the nodal flexibility matrix.

## 3. Shape Function

Divide the structure of a general tapered beam subjected to external loading and is clamped at first, middle and end into two structures as shown in Figure 6.
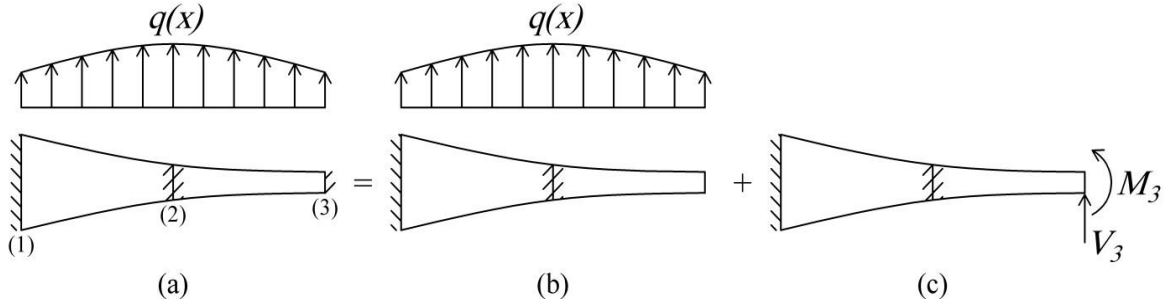


**Fig. 6. General non-prismatic beams divided into two structure (b) and (c)**

In structure (b), with regard to BDFs definitions, nodal displacement of point (3) due to external load can be calculated as followed:

$$\begin{Bmatrix} w_3 \\ \theta_3 \end{Bmatrix}^{(b)} = \int_l q(x) \begin{Bmatrix} b_{v3} \\ b_{\theta3} \end{Bmatrix} dx \qquad (19)$$

In structure (c), nodal displacement of point (3) can be calculated using flexibility matrix that:

$$\begin{Bmatrix} w_3 \\ \theta_3 \end{Bmatrix}^{(c)} = F_{33} \begin{Bmatrix} V_3 \\ M_3 \end{Bmatrix} \qquad (20)$$

By imposing the boundary conditions for displacement of point (3) we have:

$$\begin{Bmatrix} w_3 \\ \theta_3 \end{Bmatrix} = \begin{Bmatrix} w_3 \\ \theta_3 \end{Bmatrix}^{(b)} + \begin{Bmatrix} w_3 \\ \theta_3 \end{Bmatrix}^{(c)} = \begin{Bmatrix} 0 \\ 0 \end{Bmatrix} \qquad (21)$$

Substituting equations (19) and (20) into equation (21) the reactions at point 3 are obtained as:

$$\begin{Bmatrix} V_3 \\ M_3 \end{Bmatrix} = -K_{33} \int_l q(x) \begin{Bmatrix} b_{w3} \\ b_{\theta3} \end{Bmatrix} dx \qquad (22)$$

Following similar procedure, the reactions at points (1) and (2) are obtained:

$$\begin{Bmatrix} V_1 \\ M_1 \end{Bmatrix} = -K_{11} \int_l q(x) \begin{Bmatrix} b_{w1} \\ b_{\theta1} \end{Bmatrix} dx \qquad (23)$$

$$\begin{Bmatrix} V_2 \\ M_2 \end{Bmatrix} = -K_{22} \int_l q(x) \begin{Bmatrix} b_{w2} \\ b_{\theta2} \end{Bmatrix} dx \qquad (24)$$

The nodal equivalent loads which are the equal and opposite response to reactions are obtained as:

$$F = G \int_l q(x) b \, dx \qquad (25)$$

where $b$ is a vector containing BDFs ( $b^T = \{ b_{w1} \quad b_{\theta1} \quad b_{w2} \quad b_{\theta2} \quad b_{w3} \quad b_{\theta3} \}$ ).
in which:

$$G = \begin{bmatrix} K_{11} & & \\ & K_{22} & \\ & & K_{33} \end{bmatrix} \qquad (26)$$

Employing work-equivalent load method, nodal forces are given as:

$$F = \int_l q(x) N^T dx \qquad (27)$$

Shape functions can be obtained by comparing equations (25) and (27):

$$N = b^T . G \qquad (28)$$

Therefore, structural matrices, i.e. stiffness and consistent mass matrices are given as (Gallagher and Lee [3]):

$$M = \int_l N^T \rho A(x) N dx \qquad (29)$$

$$K = \int_l N^{"T} EI(x) N^{"} dx \qquad (30)$$

The structural matrices in terms of BDFs can be expressed using equations (28-30):

$$\mathbf{M} = \mathbf{G}(\int_l \mathbf{b}\rho A(x)\mathbf{b}^T dx)\mathbf{G} \qquad (31)$$

$$\mathbf{K} = \mathbf{G}(\int_l \mathbf{b}''EI(x)\mathbf{b}''^T dx)\mathbf{G} \qquad (32)$$

The application of BDFs can be clarified using a general algorithm for derivation of shape functions and structural matrices for non-prismatic beams in which each step is performed at unit length with constant cross-sectional area and moment of inertia. Obtaining BDFs using Equations (1-4) and (14-15):

$$b_{w1} = sg(0.5-x)\frac{(x+1)(2x-1)^2}{24EI}$$

$$b_{\theta1} = sg(0.5-x)\frac{-(2x-1)^2}{8EI}$$

$$b_{w2} = sg(0.5-x)\frac{(3-4x)x^2}{48EI}$$

$$b_{\theta2} = sg(0.5-x)\frac{x^2(2x-1)^2}{8EI}$$

$$b_{w3} = sg(x-0.5)\frac{-(x-2)(2x-1)^2}{24EI}$$

$$b_{\theta3} = sg(x-0.5)\frac{(2x-1)^2}{8EI}$$

The first and second derivatives of BDFs.
Derivation of nodal flexibility matrices using Equations (16-18):

$$\mathbf{F}_{11} = \frac{1}{EI}\begin{bmatrix} 0.0417 & -0.125 \\ -0.125 & 0.5 \end{bmatrix}$$

$$\mathbf{F}_{22} = \frac{1}{EI}\begin{bmatrix} 0.0052 & 0 \\ 0 & 0.0625 \end{bmatrix}$$

$$\mathbf{F}_{33} = \frac{1}{EI}\begin{bmatrix} 0.0417 & 0.125 \\ 0.125 & 0.5 \end{bmatrix}$$

Evaluating *G* using equation (29):

$$\mathbf{G} = EI\begin{bmatrix} 96 & 24 & 0 & 0 & 0 & 0 \\ 24 & 8 & 0 & 0 & 0 & 0 \\ 0 & 0 & 192 & 0 & 0 & 0 \\ 0 & 0 & 0 & 16 & 0 & 0 \\ 0 & 0 & 0 & 0 & 96 & -24 \\ 0 & 0 & 0 & 0 & -24 & 8 \end{bmatrix}$$

Derivation of shape functions using Equation (28):

$$N_1 = sg(0.5-x)(16x^3 - 12x^2 + 1)$$

$$N_2 = sg(0.5-x)(4x^3 - 4x^2 + x)$$

$$N_3 = H(0.5-x)4(3-4x)x^2 + H(0.5-x) \\ (16x^3 - 36x^2 + 24x - 4)$$

$$N_4 = H(0.5-x)2(2x-1)x^2 + H(0.5-x) \\ (4x^3 - 10x^2 + 8x - 2)$$

$$N_5 = sg(x-0.5)(-16x^3 + 36x^2 - 24x + 5)$$

$$N_6 = sg(x-0.5)(4x^3 - 8x^2 + 5x - 1)$$

where Heaviside step function ($H(x)$) is introduced in Appendix A.
Derivation of structural matrices using Equations (31) and (32):

$$K = EI\begin{bmatrix} 96 & 24 & -96 & 24 & 0 & 0 \\ & 8 & -24 & 4 & 0 & 0 \\ & & 192 & 0 & -96 & 24 \\ & & & 16 & -24 & 4 \\ & & & & 96 & -24 \\ sym. & & & & & 8 \end{bmatrix}$$

$$M = EI\begin{bmatrix} 0.1857 & 0.0131 & 0.0643 & -0.0077 & 0 & 0 \\ & 0.0012 & 0.0077 & -0.0009 & 0 & 0 \\ & & 0.3714 & 0 & 0.0643 & -0.0077 \\ & & & 0.0024 & 0.0077 & -0.0009 \\ & & & & 0.1857 & -0.0131 \\ sym. & & & & & 0.0012 \end{bmatrix}$$

## 4. Numerical Results and Discussions

In the present research, two types of numeric examples, including static analysis and free lateral vibration are discussed. The Gauss quadrature rule with 10 gauss points is used as a Numerical Integration technique. In order to describe boundary conditions, the symbolism C, S and F are utilized to identify the clamped, simply supported and free boundary conditions respectively. Except for static analysis, a uniform unit length beam is used for all numerical examples. The dimensionless natural frequency parameter, $\mu$, is used to make comparisons between the results. $\mu_i$ is defined as follows:

$$\mu_i = \omega\sqrt{\frac{\rho_0 A_0 l^4}{E_0 I_0}}$$

## 4.1. Static analysis

Three different cantilever beams, in which $L = 10m$, $E = 3 \times 10^8 kg.m$ are assumed and subjected to uniform load, $q = 1000 kg.m^{-1}$;

Vertical deflection of free the end of each case is calculated and then compared with the results obtained from classical and non-classical methods [38]. The results are tabulated in Table 1.

**Table 1. Deflection of tip due to distributed load $10^5$ N/m**

| Case | Present | Franciosi and Mecca [38] | | | | | | |
|------|---------|---------|---------|---------|---------|---------|---------|
| | | Non-classical | | | classical | | | |
| | NE=1 | NE=1 | NE =2 | NE =5 | NE =3 | NE =10 | NE =100 | NE =200 |
| A | 3.157147 | 3.15715 | 3.15715 | 3.15715 | 3.28569 | 3.16841 | 3.15726 | 3.157176 |
| B | 1.543083 | 1.54308 | 1.54308 | 1.54308 | 1.8435 | 1.56832 | 1.54333 | 1.543145 |
| C | 2.414213 | 2.41424 | 2.41422 | 2.41421 | 2.99927 | 2.46085 | 2.414674 | 2.414329 |

The comparison shows that using the present method is more efficient in the static analysis. The three different cantilever beam cases are specified as follows:

Case A) unit depth, width is defined as:
$b = 2 - 0.175x$

Case B) unit width, depth is defined as:
$h = 2 - 0.175x$

Case C) unit width, depth is defined as:
$h = \left(\sqrt{2} + (0.05 - 0.1\sqrt{2})x\right)^2$

The vertical displacement is obtained using a single finite element with varying cross section and is reported in the second column.

## 4.2. Free lateral vibration

**Example 1.**

Consider a cantilever beam, in which the cross-section and moment of inertia vary as follows:

$$A(\xi) = A_0 (1 - c\xi)^n$$

$$I(\xi) = I_0 (1 - c\xi)^{n+2}$$

where $\xi = x/L$

Different values of $n$ indicate the distinctive applications of the beam. For example, when $n$ is set to two, the beam is applicable for beams with circular cross-section whose diameter varies linearly or for beams whose height and breadth both vary linearly with the same taper Raito. In order to investigate the efficiency of the method, the first three natural frequencies and special cases of $n = 1$ and $n = 2$ are compared with those of Banerjee *et al.* [15] and Attarnejad [31]. The results are tabulated in Table 2 and Table 3.

**Table 2. The first three non-dimensional transverse frequencies ( $\mu_i = \omega_i \sqrt{\rho_0 A_0 l^4 / E_0 I_0}$ ) of a tapered beam (NE=12)**

| | c | 0.1 | 0.2 | 0.3 | 0.4 | 0.5 | 0.6 | 0.7 | 0.8 | 0.9 |
|---|---|---|---|---|---|---|---|---|---|---|
| $\mu_1$ | Present | 3.5587 | 3.60828 | 3.66675 | 3.73708 | 3.82379 | 3.93429 | 4.08171 | 4.2925 | 4.63073 |
| | Attarnejad [31] | 3.5587 | 3.60828 | 3.66675 | 3.73708 | 3.82379 | 3.93429 | 4.08173 | 4.29252 | 4.63079 |
| | Banerjee *et al.* [15] | 3.5587 | 3.60827 | 3.66675 | 3.73708 | 3.82379 | 3.93428 | 4.08171 | 4.29249 | 4.63073 |
| $\mu_2$ | Present | 21.3381 | 20.621 | 19.8806 | 19.1138 | 18.3173 | 17.4879 | 16.6253 | 15.7428 | 14.931 |
| | Attarnejad [31] | 21.3385 | 20.6214 | 19.881 | 19.1142 | 18.3177 | 17.4884 | 16.6259 | 15.7437 | 14.9332 |
| | Banerjee *et al.* [15] | 21.3381 | 20.621 | 19.8806 | 19.1138 | 18.3173 | 17.4878 | 16.6252 | 15.4727 | 14.9308 |
| $\mu_3$ | Present | 58.9804 | 56.1927 | 53.3227 | 50.3541 | 47.2653 | 44.0253 | 40.5884 | 36.8853 | 32.8346 |
| | Attarnejad [31] | 58.9874 | 56.1996 | 53.3294 | 50.3609 | 47.2722 | 44.0326 | 40.5966 | 36.8957 | 32.8538 |
| | Banerjee *et al.* [15] | 58.9799 | 56.1923 | 53.3222 | 50.3537 | 47.2649 | 44.0248 | 40.5879 | 36.8846 | 32.8331 |

**Table 3. The first three non-dimensional transverse frequencies ( $\mu_i = \omega_i \sqrt{\rho_0 A_0 l^4 / E_0 I_0}$ ) of a tapered beam (NE=12)**

| | c | 0.1 | 0.2 | 0.3 | 0.4 | 0.5 | 0.6 | 0.7 | 0.8 | 0.9 |
|---|---|---|---|---|---|---|---|---|---|---|
| $\mu_1$ | Present | 3.6737 | 3.85512 | 4.06693 | 4.31878 | 4.62515 | 5.00903 | 5.50926 | 6.1964 | 7.20488 |
| | Attarnejad [31] | 3.6737 | 3.85512 | 4.06694 | 4.31878 | 4.62516 | 5.00905 | 5.50929 | 6.19646 | 7.20506 |
| | Banerjee *et al.* [15] | 3.6737 | 3.85511 | 4.06694 | 4.31878 | 4.62515 | 5.00904 | 5.50926 | 6.19639 | 7.20488 |
| $\mu_2$ | Present | 21.5503 | 21.0568 | 20.5555 | 20.05 | 19.5476 | 19.0649 | 18.6412 | 18.3856 | 18.6805 |
| | Attarnejad [31] | 21.5506 | 21.0571 | 20.5559 | 20.0505 | 19.5482 | 19.0656 | 18.6422 | 18.3872 | 18.6848 |
| | Banerjee *et al.* [15] | 21.5503 | 21.0568 | 20.5555 | 20.05 | 19.5476 | 19.0649 | 18.6412 | 18.3855 | 18.6803 |
| $\mu_3$ | Present | 59.1891 | 56.6308 | 54.0157 | 51.3351 | 48.5794 | 45.7389 | 42.8111 | 39.8346 | 37.1261 |
| | Attarnejad [31] | 59.1962 | 56.6379 | 54.0227 | 51.3423 | 48.587 | 45.7472 | 42.8209 | 39.8485 | 37.1573 |
| | Banerjee *et al.* [15] | 59.1886 | 56.6303 | 54.0152 | 51.3346 | 48.5789 | 45.7384 | 42.8104 | 39.8336 | 37.1241 |

Table 4 is tabulated for fourth and fifth natural frequencies and specified taper ratio c=0.5.

**Table 4. The effect of this element on higher frequencies**

| | n=1 | | n=2 | |
|---|---|---|---|---|
| | $\mu_4$ | $\mu_5$ | $\mu_4$ | $\mu_5$ |
| Present(NE=12) | 90.4537 | 148.016 | 91.8162 | 149.404 |
| Banerjee *et al.* [15] | 90.4505 | 148.002 | 91.8128 | 149.39 |

The effect of this element on taper ratios higher than 0.9 are presented in Table 5.

**Table 5. The effect of this element on higher taper ratios**

| | NE=20 | n=1 | | n=2 | |
|---|---|---|---|---|---|
| | | c=0.99 | c=0.995 | c=0.99 | c=0.995 |
| $\mu_1$ | Present | 5.21446 | 5.26321 | 8.54601 | 8.62732 |
| | Banerjee *et al.* [15] | 5.21445 | 5.26337 | 8.54601 | 8.63232 |
| $\mu_2$ | Present | 14.9672 | 15.0708 | 20.7302 | 20.8613 |
| | Banerjee *et al.* [15] | 14.967 | 15.0722 | 20.7301 | 20.9355 |
| $\mu_3$ | Present | 29.7292 | 29.8062 | 37.7284 | 37.7216 |
| | Banerjee *et al.* [15] | 29.7265 | 29.8064 | 37.7253 | 38.0742 |
| $\mu_4$ | Present | 49.7144 | 49.5695 | 59.6492 | 59.2879 |
| | Banerjee *et al.* [15] | 49.6986 | 49.5473 | 59.6278 | 60.0908 |

**Example 2.**

Consider a beam of constant depth whose cross-sectional area and moment of inertia respectively vary as:

$$A = e^{\delta\xi} \;, I = e^{\delta\xi}$$

The first three natural frequencies for SS and CC boundary conditions and a given non-uniformity parameter, $\delta$, are determined and compared with those of Ece et al. [12]. Furthermore, the first five natural frequencies for CF boundary condition and non-uniformity parameter $\delta = -1$, are determined and compared with those of Attarnejad et al. [37]. Cranch and Adeer [39]. Ece et al. [12] and Tong and Tabarrok [40]. The results are tabulated in Table 6 and Table 7.

**Table 6. The effect of number of elements on accuracy of dimensionless natural frequencies for and different taper ratios and boundary conditions**

| $\delta$ | Mode number | SS | | | CC | | |
|---|---|---|---|---|---|---|---|
| | | Present | | Ece *et al.* [12] | Present | | Ece *et al.* [12] |
| | | NE=10 | NE=20 | | NE=10 | NE=20 | |
| 0 | 1 | 9.86961 | 9.8696 | 9.8696 | 22.37333 | 22.37329 | 22.37327 |
| | 2 | 39.47868 | 39.47843 | 39.47841 | 61.673838 | 61.67289 | 61.67281 |
| | 3 | 88.82946 | 8.882663 | 88.82643 | 120.91101 | 120.90387 | 120.90338 |
| | 4 | 157.93057 | 157.91474 | 157.91367 | 199.89368 | 199.86161 | 199.85945 |
| | 5 | 246.80417 | 246.74416 | 246.74011 | 298.6689 | 298.56272 | 298.55552 |
| 1 | 1 | 9.77291 | 9.77291 | 9.77291 | 22.51173 | 22.51168 | 22.51167 |
| | 2 | 39.57063 | 39.57038 | 39.57036 | 61.86072 | 61.85976 | 61.85968 |
| | 3 | 88.97356 | 88.97071 | 88.97052 | 121.11564 | 121.10847 | 121.10799 |
| | 4 | 158.10114 | 158.08526 | 158.08418 | 200.10846 | 200.07628 | 200.07411 |
| | 5 | 246.99071 | 246.93057 | 246.9265 | 298.89023 | 298.78382 | 298.77661 |

**Table 7. Dimensionless natural frequencies of the beam in Example 2 ($\delta$= -1).**

| Mode number | Present (NE=20) | Attarnejad *et al.* [37] | Cranch and Adler [39] | Tong and Tabarrok [40] | Ece *et al.* [12] |
|---|---|---|---|---|---|
| 1 | 4.7349 | 4.7349 | 4.735 | 4.7347 | 4.72298 |
| 2 | 24.20187 | 24.2018 | 24.2025 | 24.2005 | 24.20168 |
| 3 | 63.86561 | 63.8645 | 63.85 | 63.8608 | 63.86448 |
| 4 | 123.10588 | 123.098 | - | 123.91 | 123.0979 |
| 5 | 202.10378 | - | - | - | 202.0687 |

Tables 2 to 7 show that the predicted results by the present element are in good agreement with results obtained from previous method. In example 1, unlike the first mode the second and third modes decrease with increased taper ratio, which is due to the softening effect resulting from the reduction in cross-sectional area and moment of inertia. It is worth mentioning that with the equal number of elements, 3-node method yields more accurate results than 2-node method. In example 1 and 2, the results are acceptable for taper ratios upper than 0.9, higher frequencies and different boundary conditions. Figure 7 is plotted in order to show the effects of taper ratios on all six shape functions. It is observed that the effect of taper ratio is clearly reflected in shape functions.

$N_1$

$N_2$

$N_3$

$N_4$

$N_5$

$N_6$
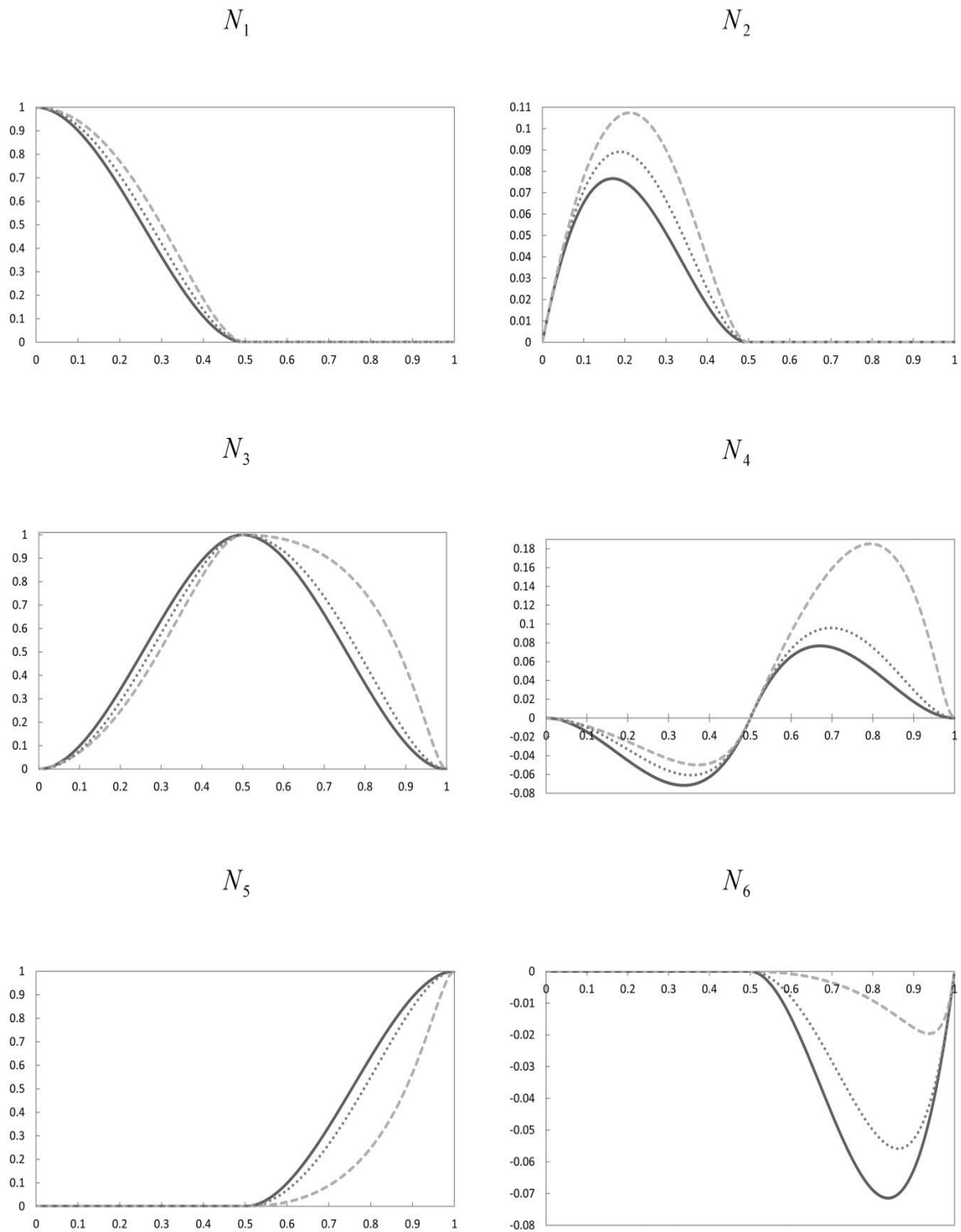
**Fig. 7. Variation of shape function of beam element of unit length for example 1 and n=2 (solid line: C=0.1, Dotted line C=0.5, Dashed line: C=0.9)**

In order to compare convergence between 3-node method and 2-node method, Figure 8 are plotted for a cantilever beam with $A = e^{0.5\xi}$, $I = e^{0.5\xi}$

of elements in 3-node method, the speed of convergence increases remarkably.

The results obtained from Banerjee *et al.* [15] are assumed as exact solution to calculate the error. Figure 9 illustrates the error concerning of third mode frequency in example 2. The figure indicates that as the number of elements and taper ratio increase, the errors are in a similar range and consequently, the element stays stable.
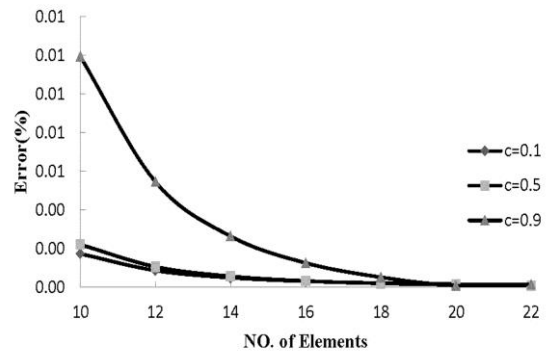


**Fig. 9. Error concerning of third mode frequency with respect to number of elements**

Finally, benchmark example is provided. In this example, it is assumed that

$$A(\xi) = A_0 \left(1 - c_b\xi\right)\left(1 - c_h\xi\right)^2$$

$$I(\xi) = I_0 \left(1 - c_b\xi\right)\left(1 - c_h\xi\right)^4$$

where $c_b$ and $c_h$ are taper ratios. In order to facilitate the presentation of benchmark results, non-dimensional parameters are introduced in Table 8.

**Fig. 8. Convergence of non-dimensional transverse frequencies of cantilever beam (0.5) and compare with 2-node method (solid line: 3-node, Dashed line: 2-node)**

It is observed that utilizing fewer numbers

**Table 8. First three non-dimensional transverse frequencies of non-prismatic Euler-Bernoulli beam**

| | NE | $C_b$ / $C_h$ | 0 | | | 0.3 | | | 0.6 | | | 0.9 | | |
|---|---|---|---|---|---|---|---|---|---|---|---|---|---|---|
| | | | $\mu_1$ | $\mu_2$ | $\mu_3$ | $\mu_1$ | $\mu_2$ | $\mu_3$ | $\mu_1$ | $\mu_2$ | $\mu_3$ | $\mu_1$ | $\mu_2$ | $\mu_3$ |
| S-S | 10 | 0 | 9.8696 | 39.4787 | 88.8295 | 9.8574 | 39.4899 | 88.8474 | 9.7946 | 39.5384 | 88.9357 | 9.5441 | 39.5586 | 89.1311 |
| | | 0.3 | 8.2502 | 33.4015 | 75.712 | 8.1783 | 33.4706 | 75.1792 | 8.0337 | 33.6009 | 75.3938 | 7.6541 | 33.7651 | 75.8167 |
| | | 0.6 | 6.2086 | 26.852 | 59.9938 | 6.0815 | 26.9886 | 60.1969 | 5.8609 | 27.224 | 60.5545 | 5.3579 | 27.6062 | 61.2759 |
| | | 0.9 | 3.0513 | 19.0941 | 41.4977 | 2.9038 | 19.3619 | 41.8282 | 2.6604 | 19.8372 | 42.4141 | 2.1299 | 20.8582 | 43.805 |
| | 20 | 0 | 9.8696 | 39.4784 | 88.8266 | 9.8574 | 39.4896 | 88.8446 | 9.7946 | 39.5382 | 88.9328 | 9.5441 | 39.5584 | 89.1283 |
| | | 0.3 | 8.2502 | 33.4013 | 75.0687 | 8.1783 | 33.4704 | 75.1767 | 8.0337 | 33.6007 | 75.3913 | 7.6541 | 33.7649 | 75.8141 |
| | | 0.6 | 6.2086 | 26.8518 | 59.9915 | 6.0815 | 26.9884 | 60.1945 | 5.8609 | 27.2238 | 60.5521 | 5.3579 | 27.606 | 61.2734 |
| | | 0.9 | 3.0513 | 19.0938 | 41.494 | 2.9038 | 19.3616 | 41.8245 | 2.6604 | 19.8368 | 42.4103 | 2.1299 | 20.8579 | 43.8008 |
| C-C | 10 | 0 | 22.3733 | 61.6738 | 120.911 | 22.3213 | 61.6028 | 120.8329 | 22.0465 | 61.2143 | 120.3964 | 20.784 | 59.168 | 117.8486 |
| | | 0.3 | 18.9233 | 52.0864 | 102.05 | 18.9974 | 52.1866 | 102.16 | 18.9399 | 52.1027 | 102.0642 | 18.1829 | 50.8513 | 100.4863 |
| | | 0.6 | 15.1898 | 41.4773 | 80.9834 | 15.4008 | 41.7544 | 81.2861 | 15.5863 | 41.9997 | 81.5565 | 15.4136 | 41.658 | 81.0894 |
| | | 0.9 | 10.7636 | 28.2362 | 54.1083 | 11.1752 | 28.719 | 54.6245 | 11.7312 | 29.3891 | 55.3494 | 12.4914 | 30.4 | 56.4982 |

**Table 8. First three non-dimensional transverse frequencies of non-prismatic Euler-Bernoulli beam (continue)**

| | NE | $C_b$ / $C_h$ | 0 | | | 0.3 | | | 0.6 | | | 0.9 | | |
|---|---|---|---|---|---|---|---|---|---|---|---|---|---|---|
| | | | $\mu_1$ | $\mu_2$ | $\mu_3$ | $\mu_1$ | $\mu_2$ | $\mu_3$ | $\mu_1$ | $\mu_2$ | $\mu_3$ | $\mu_1$ | $\mu_2$ | $\mu_3$ |
| C-C | 20 | 0 | 22.3733 | 61.6729 | 120.904 | 22.3213 | 61.6019 | 120.8258 | 22.0465 | 61.2134 | 120.3894 | 20.784 | 59.1671 | 117.842 |
| | | 0.3 | 18.9232 | 52.0856 | 102.044 | 18.9974 | 52.1857 | 102.1539 | 18.9398 | 52.1019 | 102.058 | 18.1829 | 50.8506 | 100.4805 |
| | | 0.6 | 15.1898 | 41.4766 | 80.9779 | 15.4007 | 41.7536 | 81.2805 | 15.5862 | 41.9989 | 81.5509 | 15.4135 | 41.6572 | 81.0838 |
| | | 0.9 | 10.7636 | 28.2353 | 54.1012 | 11.1752 | 28.7181 | 54.6172 | 11.7312 | 29.3881 | 55.3417 | 12.4914 | 30.3989 | 56.4902 |
| C-F | 10 | 0 | 3.516 | 22.0345 | 61.6982 | 3.916 | 22.786 | 62.4372 | 4.5853 | 24.0211 | 63.7526 | 6.0704 | 27.299 | 68.1159 |
| | | 0.3 | 4.0669 | 20.5556 | 54.0162 | 4.5004 | 21.2539 | 54.746 | 5.2231 | 22.4097 | 56.0114 | 6.8148 | 25.5282 | 60.0635 |
| | | 0.6 | 5.009 | 19.065 | 45.7396 | 5.4889 | 19.7173 | 46.4495 | 6.2816 | 20.8063 | 47.6543 | 7.994 | 23.7956 | 51.3851 |
| | | 0.9 | 7.2049 | 18.6808 | 37.1285 | 7.7631 | 19.3087 | 37.8012 | 8.6463 | 20.3767 | 38.946 | 10.388 | 23.3075 | 42.4561 |
| | 20 | 0 | 3.516 | 22.0345 | 61.6973 | 3.916 | 22.786 | 62.4362 | 4.5853 | 24.0211 | 63.7515 | 6.0704 | 27.2989 | 68.1146 |
| | | 0.3 | 4.0669 | 20.5555 | 54.0153 | 4.5004 | 21.2538 | 54.745 | 5.2231 | 22.4096 | 56.0104 | 6.8148 | 25.5281 | 60.0622 |
| | | 0.6 | 5.009 | 19.0649 | 45.7384 | 5.4889 | 19.7172 | 46.4483 | 6.2816 | 20.8062 | 47.6531 | 7.994 | 23.7955 | 51.3834 |
| | | 0.9 | 7.2049 | 18.6802 | 37.1241 | 7.763 | 19.3081 | 37.7965 | 8.6462 | 20.376 | 38.9409 | 10.3879 | 23.3065 | 42.4494 |
| C-S | 10 | 0 | 15.4182 | 49.9654 | 104.253 | 15.7687 | 50.2939 | 104.5828 | 16.1948 | 50.7029 | 105.0124 | 16.6372 | 51.1485 | 105.6097 |
| | | 0.3 | 13.9617 | 43.1283 | 88.9422 | 14.2939 | 43.5113 | 89.3501 | 14.7019 | 44.0033 | 89.8955 | 15.1302 | 44.6113 | 90.7173 |
| | | 0.6 | 12.2329 | 35.5595 | 71.8982 | 12.5739 | 35.9984 | 72.3812 | 13.0088 | 36.5866 | 73.05 | 13.5171 | 37.4217 | 74.1576 |
| | | 0.9 | 9.9086 | 26.1094 | 50.3911 | 10.353 | 26.632 | 50.9559 | 10.9793 | 27.3998 | 51.8011 | 11.9495 | 28.8143 | 53.5177 |
| | 20 | 0 | 15.4182 | 49.9649 | 104.248 | 15.7686 | 50.2934 | 104.5782 | 16.1948 | 50.7024 | 105.0077 | 16.6372 | 51.1479 | 105.605 |
| | | 0.3 | 13.9617 | 43.1279 | 88.9381 | 14.2939 | 43.5108 | 89.3459 | 14.7019 | 44.0028 | 89.8912 | 15.1302 | 44.6108 | 90.7129 |
| | | 0.6 | 12.2328 | 35.559 | 71.8942 | 12.5738 | 35.9979 | 72.3771 | 13.0087 | 36.5861 | 73.0458 | 13.517 | 37.4211 | 74.1532 |
| | | 0.9 | 9.9086 | 26.1087 | 50.3846 | 10.353 | 26.6311 | 50.9491 | 10.9793 | 27.3989 | 51.794 | 11.9495 | 28.8133 | 53.51 |

## 5. Conclusions

A flexibility-based method for static and dynamic analysis of non-prismatic Euler-Bernoulli beams has been presented. The main aspects of new approach are:

1. Introduction of 3-node BDFs.
2. All types of cross-sections and cross-sectional dimensions of the beam element could be considered in this method.
3. Shape functions for any type of cross sectional properties could be obtained for that type.
4. Although the new shape functions are derived based on static deformations, they were employed in the dynamic analysis, satisfactory results were obtained for natural frequencies even for a coarse mesh.
5. The new element provides better results with the same mesh in upper frequencies and different boundary conditions than 2-node element.
6. The method can be extended to analysis of curved beams as well as shells of revolution.
7. The method can be used for analysis of straight and curved Timoshenko beam elements.
8. The method is being extended to analysis of plates and shells.

## Appendix A

Heaviside step function was defined as:

$$H(y) = \begin{cases} 0 & y < 0 \\ \dfrac{1}{2} & y = 0 \\ 1 & y > 0 \end{cases}$$

## References

[1]. Gunda J.B., Ganguli R., 2008, New rational interpolation functions for finite element analysis of rotating beams, Int. J. Mech. Sci. **50:** 578-588.

[2]. Caruntu D.I., 2009, Dynamic modal characteristics of transverse vibrations of cantilevers of parabolic thickness, Mech. Res. Commun. **36:** 391–404.

[3]. Gallagher R.H., Lee C.H., 1970, Matrix dynamic and instability analysis with non-uniform elements, J. Numer. Meth. Eng. **2:** 265-275.

[4]. Karabalis D.L., Beskos D.E., 1983, Static, dynamic and stability analysis of structures

composed of tapered beams, Comput. Struct. **16:** 731-748.

[5]. Eisenberger M., Reich Y., 1989, Static, vibration and stability analysis of non-uniform beams, Comput. Struct. **31:** 563-571.

[6]. Eisenberger M., 1986, An exact element method, Int. J. Numer. Meth. Eng. **30:** 363-370.

[7]. Eisenberger M., 1991, Exact solution for general variable cross-section members, Comput. Struct. **41:** 765-772.

[8]. Banerjee J.R., Williams F.W., 1985, Exact Bernoulli-Euler dynamic stiffness matrix for a range of tapered beam, J. Numer. Meth. Eng. **21:** 2289-2302.

[9]. Mou Y., Han R.S.P., Shah A.H., 1997, Exact dynamic stiffness matrix for beams of arbitrarily varying cross sections, Int. J. Numer. Meth. Eng. **40:** 233-250.

[10]. Chambers J.J., Almudhafar S., Stenger F., 2003, Effect of reduced beam section frame elements on stiffness of moment frames, J. Struct. Eng. **129:** 383-393.

[11]. Kim K.D., Engelhardt M.D., 2007, Nonprismatic beam element for beams with RBS connections in steel moment frames, J. Struct. Eng. **133:** 176-184.

[12]. Ece M.C., Aydogdu M., Taskin V., 2007, Vibration of a variable cross-section beam, Mech. Res. Commun. **34:** 78-84.

[13]. Banerjee J.R., 2000, Free vibration of centrifugally stiffened uniform and tapered beams using the dynamic stiffness method. J. Sound Vib. **233:** 857-875.

[14]. Wang G., Wereley N.M., 2004, Free vibration analysis of rotating blades with uniform tapers, J. AIAA **42:** 2429-2437.

[15]. Banerjee J.R., Su H., 2006, Jackson D.R., Free vibration of rotating tapered beams using the dynamic stiffness method, J. Sound Vib. **298:** 1034-1054.

[16]. Ruta P., 1999, Application of Chebyshev series to solution of non-prismatic beam vibration problems, J. Sound Vib. **227:** 449-467.

[17]. Auciello N.M., Ercolano A., 2004, A general solution for dynamic response of axially loaded non-uniform Timoshenko beams, Int. J. Solids Struct. **41:** 4861–4874.

[18]. Ho S.H., Chen C.K., 1998, Analysis of general elastically end restrained non-uniform beams using differential transform, Appl. Math. Model. **22:** 219–234.

[19]. Zeng H., Bert C.W., 2001, Vibration analysis of a tapered bar by differential transformation, J. Sound Vib. **242:** 737–739.

[20]. Ozdemir O., Kaya M.O., 2006, Flapwise bending vibration analysis of a rotating tapered cantilever Bernoulli–Euler beam by differential transform method, J. Sound Vib. **289:** 413–420.

[21]. Ozdemir O., Kaya M.O., 2006, Flapwise bending vibration analysis of double tapere rotating Euler–Bernoulli beam by using the differential transform method, Meccanica **40:** 661–670.

[22]. Seval C., 2008, Solution of free vibration equations of beam on elastic soil by using differential transform method, Appl. Math. Model **32:** 1744-1757.

[23]. Balkaya M., Kaya M.O., Saglamer A., 2009, Analysis of the vibration of an elastic beam supported on elastic soil using the differential transform method, Arch. Appl. Mech. **79:** 135–146.

[24]. Catal S., 2008, Solution of free vibration equations of beam on elastic soil by using differential transform method, Appl. Math. Model. **32:** 1744–1757.

[25]. Yesilce Y., Catal S., 2009, Free vibration of axially loaded Reddy-Bickford beam on elastic soil using the differential transform method, Struct. Eng. Mech. **31:** 453–476.

[26]. Yesilce Y., 2010, DTM and DQEM for free vibration of axially loaded and semi-rigid-connected Reddy-Bickford beam, Commun. Numer. Meth. Eng. **27:** 666-693.

[27]. Attarnejad R., Shahba A., 2008, Application of differential transform method in free vibration analysis of rotating non-prismatic beams, World Appl. Sci. J. **5:** 441-448.

[28]. Shahba A., Rajasekaran S., 2012, Free vibration and stability of tapered Euler-Bernoulli beams made of axially functionally graded materials, Appl. Math. Model. **36:** 3094-3111.

[29]. Attarnejad R., 2000, On the derivation of the geometric stiffness and consistent mass matrices for non-prismatic Euler-Bernoulli beam elements, Barcelona, Proceedings of European Congress on Computational Methods in Applied Sciences and Engineering.

[30]. Attarnejad R., 2002, Free vibration of non-prismatic beams, New York, Proceedings of 15th ASCE Engineering Mechanics Conference.

[31]. Attarnejad R., 2010, Basic displacement functions in analysis of non-prismatic beams, Eng. Comput. **27:** 733-776.

[32]. Attarnejad R., Shahba A., 2011, Basic displacement functions in analysis of centrifugally stiffened tapered beams, AJSE **36:** 841-853.

[33]. Attarnejad R., Shahba A., Semnani S.J., 2011, Analysis of non-prismatic Timoshenko beams using basic displacement functions, Adv. Struct. Eng. **14:** 319-332.

[34]. Attarnejad R., Shahba A., 2010, Dynamic basic displacement functions in free vibration analysis of centrifugally stiffened tapered

beams; a mechanical solution, Meccanica **46:** 1267-1281.

[35]. Attarnejad R., Shahba A., 2011, Basic displacement functions for centrifugally stiffened tapered beams, Commun. Numer. Meth. Eng. **27:** 1385-1397.

[36]. Attarnejad R., Semnani S.J., Shahba A., 2010, Basic displacement functions for free vibration analysis of non-prismatic Timoshenko beams, Finite Elem. Anal. Des. **46:** 916-929.

[37]. Attarnejad R., Shahba A., Eslaminia M., 2011, Dynamic basic displacement functions for free vibration analysis of tapered beams, J. Vib. Control **17:** 2222-2238.

[38]. Franciosi C., Mecca M., 1998, Some finite elements for the static analysis of beams with varying cross section, Comput. Struct. **69:** 191-196.

[39]. Cranch E.T., Adler A.A., 1956, Bending vibration of variable section beams, J. Appl. Mech. **23:** 103–108.

[40]. Tong X., Tabarrok B., 1995, Vibration analysis of Timoshenko beams with non-homogeneity and varying cross-section, J. Sound Vib. **186:** 821–835.

**Nomenclature**

$l$ beam length

$b_{u1}, b_{w1}, b_{\theta1}, b_{u2}, b_{w2}, b_{\theta2}, b_{u3}, b_{w3}, b_{\theta3}$
basic displacement functions

$\mu_i$ non-dimensional transverse natural frequencies

$c$ taper ratio

$\mathbf{F_{11}}$ nodal flexibility matrix of the left node

$\mathbf{F_{22}}$ nodal flexibility matrix of the mid node

$\mathbf{F_{33}}$ nodal flexibility matrix of the right node

$x$ longitudinal coordinate

$NE$ total number of beam elements

$I_0$ moment of inertia at origin

$\mathbf{b}'_w, \mathbf{b}''_w$ first and second derivative of $\mathbf{b_w}$ with respect to $x$

$\mathbf{K_{11}}$ nodal stiffness matrix of the left node

$\mathbf{K_{22}}$ nodal stiffness matrix of the mid node

$\mathbf{K_{33}}$ nodal stiffness matrix of the right node

$\mathbf{F}$ equivalent nodal forces

$\mathbf{G}$ matrix containing nodal flexural stiffness matrices

$E_0$ modulus of elasticity at origin

$\rho_0$ mass density at origin

$A_0$ cross-sectional area at origin

$\mathbf{M}$ element consistent mass matrix

$\mathbf{N}$ shape functions

$\mathbf{N}', \mathbf{N}''$ first and second derivative of $\mathbf{N}$ with respect to $x$